Journal of Magnetic Resonance **143,** 213–216 (2000)
doi:10.1006/jmre.1999.2000, available online at http://www.idealibrary.com on IDEAL®

Temperature-Dependent Chemical Shift and Relaxation Times of ^{23}Na in $Na_4HTm[DOTP]$

Erik M. Shapiro,* Arijitt Borthakur,† Navin Bansal,† John S. Leigh,† and Ravinder Reddy†

**Department of Chemistry and †Department of Radiology, University of Pennsylvania, Philadelphia, Pennsylvania 19104*

Received July 7, 1999; revised December 15, 1999

We describe the characterization of a ^{23}Na temperature-dependent chemical shift and relaxation rates in the complex, $Na_4HTm[DOTP]$. This is the first characterization of a ^{23}Na temperature-dependent chemical shift in a nonmetallic sample. The ^{23}Na temperature-dependent chemical shift coefficient is ~ -0.5 PPM/°C for both an aqueous solution and a 6% agarose gel of this compound. This is 50 times the magnitude of the temperature-dependent chemical shift coefficient of water protons. The relaxation times, T_1, T_{2f}, and T_{2s} increased by 0.1, 0.01, and 0.05 ms/°C, respectively. Applications of these unique properties for designing an MRI technique for monitoring heat deposition in tissue and tissue phantoms are discussed. © 2000 Academic Press

Key Words: **^{23}Na; temperature mapping; temperature-dependent chemical shift; RF heating.**

NMR temperature monitoring has many direct uses in medicine and diagnostic magnetic resonance imaging (MRI). These include aiding in the use of hyperthermia for cancer treatment (*1–4*), diagnosing metabolic abnormalities (*5*), and studying muscle exercise and recovery (*6*). This has been accomplished using numerous methods, including monitoring the chemical shift and relaxation rates of water (*5, 7–9*), molecular diffusion rate changes (*1, 10*), and the chemical shift and relaxation rates of certain paramagnetic lanthanide complexes (*11–15*). Analogous techniques that employ the use of thermocouples are limited by resolution and their invasive nature, presenting problems for both the subject and the operator. The most important characteristics of an NMR method for monitoring temperature must be rapidly generated high-resolution maps and a large temperature sensitivity with minimal influence from local motion and susceptibility variations. Unfortunately, the frequency shift of water protons is only on the order of -0.01 ppm/°C, with a T_1 (longitudinal relaxation time) difference of $\sim 1.5\%$/°C. Chemical shift and relaxation rate changes of water have been used to measure temperature changes in numerous studies; however, the main limitation with these methods has been low sensitivity to small changes in temperature. While some success has been achieved using these properties to monitor temperature, the properties exhibited by the paramagnetic lanthanide complexes provide much greater temperature sensitivity. In this communication we report the temperature-dependent NMR properties of ^{23}Na in thulium(III)-1,4,7,10-tetraazacyclododecane-1,4,7,10-tetrakis(methylene phosphonate), tetrasodium salt ($Na_4HTm[DOTP]$) (Macrocyclics, Dallas, TX). We have discovered a temperature-dependent chemical shift coefficient of -0.5 PPM/°C and temperature-dependent relaxation times of 0.1 ms/°C.

Paramagnetic lanthanide complexes have been used in NMR since the 1970s as shift reagents. Recently, they have been used as sodium shift reagents in living systems (*16*), allowing the discrimination of intra- and extracellular sodium pools. Several paramagnetic lanthanide complexes have been shown to have temperature-dependent chemical shifts of one or more of its resonance peaks (and peaks of the solution in which they are incorporated) (*11–15*). The proton and phosphorous chemical shifts and relaxation rates of $Tm[DOTP]^{5-}$ as a function of temperature have previously been reported (*11, 13*). The ^{31}P temperature-dependent chemical shift coefficient of the phosphonate groups on the macrocycle is 2.18 ppm/°C and it is between 0.42 and 2.88 ppm/°C for the various protons. ^1H T_1's and T_2's (transverse relaxation time) are extremely short, on the order of 1.7 ms or less, with ^{31}P T_1 and T_2 near 3 ms. This is due to the extreme proximity of these atoms with the highly paramagnetic thulium. There is a minor effect of temperature increase on both T_1 and T_2.

Our investigation was based on four sample types. Two samples contained 40 mM $Na_4HTm[DOTP]$, one as a solution in doubly deionized water and the other in a 6% agarose gel. Two other samples contained 160 mM NaCl, again with one as a solution in doubly deionized water and the other in a 6% agarose gel. The pH of the solutions did not change upon addition of the agarose. All experiments were carried out at 9.4 T where ^{23}Na resonates at a frequency of 107.07 MHz. Sample heating was accomplished inside the magnet with a Bruker variable temperature unit. ^{23}Na exhibits biexponential T_1 and T_2 behavior when motional narrowing is not achieved, such as in a gel. Due to the small difference between the two T_1's, we employed a standard inversion recovery method to obtain a value for T_1. Multiple quantum filtering (MQF) methods are well suited to measuring two T_2's (T_{2f}, fast relaxation time, and T_{2s}, slow relaxation time) (*17, 18*). The MQF pulse sequence we employed is

1090-7807/00 $35.00
Copyright © 2000 by Academic Press
All rights of reproduction in any form reserved.

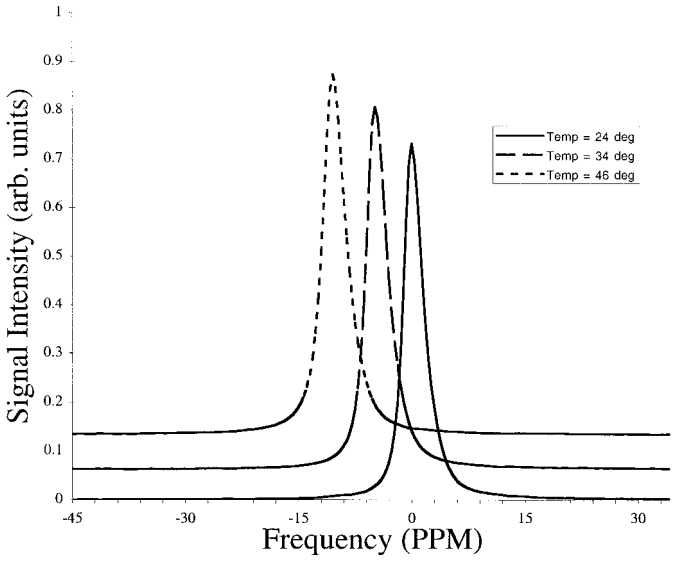

FIG. 1. Three ^{23}Na spectra of the gel sample at three different temperatures. The solid line is the spectrum taken at 24°C, the broken line is the spectrum taken at 34°C, and the dashed line is the spectrum taken at 46°C. The spectra are vertically offset for presentation purposes. The spectrum at 46°C is shifted nearly −11 PPM from the reference peak at 24°C.

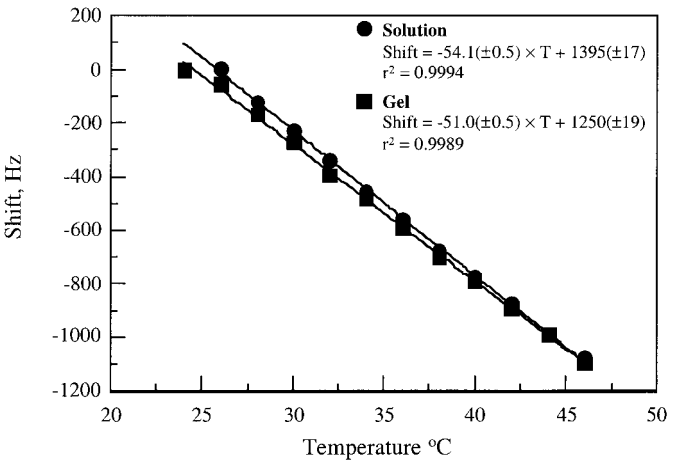

FIG. 2. Plot of temperature versus chemical shift for both the agarose gel and the solution samples. The agarose gel sample is represented by the squares and the solution sample is represented by the circles. The chemical shift coefficient is the slope of the line divided by the resonant frequency for ^{23}Na at 9.4 T (107.07 MHz). For the solution sample, the chemical shift coefficient is −54.1 ± 0.5 Hz or −0.51 ± 0.01 PPM/°C. The agarose gel sample has a chemical shift coefficient of −51.0 ± 0.5 Hz or −0.48 ± 0.01 PPM/°C.

$$(\pi/2)_{\phi 1}-\tau/2-(\pi)_{\phi 2}-\tau/2-(\pi/2)_{\phi 3}-\delta-(\pi/2)_{\phi 4}-t,$$

where ϕ is the phase of the radiofrequency (RF) pulse, τ is the preparation time, δ is the evolution time, and t is the detection time. With appropriate phase cycling, either double quantum filtering or triple quantum filtering is achieved (*19*). All data processing was performed offline on a SGI O2 using Interactive Data Language (Boulder, CO).

To determine the temperature coefficient of the sodium chemical shift for $Na_4HTm[DOTP]$, each sample was heated from room temperature (24°C for the gel, 26°C for the solution) to 46°C in steps of 2°C. Ten minutes were allowed for equilibration of the sample after the temperature monitor had already read the correct temperature. To verify complete equilibration of the temperature, linewidths of the individual spectra were calculated at each temperature. Incomplete equilibration would result in an increase in linewidth, because the peak would shift during signal averaging, yielding a broadened signal. We found the linewidths of the peaks to be invariant at all temperatures. Representative ^{23}Na spectra of the gel sample at three different temperatures are shown in Fig. 1.

Figure 2 displays the plot of chemical shift versus temperature from both the $Na_4HTm[DOTP]$ solution and the agarose gel samples. The slopes of the lines reflect the temperature-dependent chemical shift coefficient in Hz/°C. The gel sample has a temperature coefficient of −51.0 ± 0.5 Hz/°C while the solution sample has a coefficient of −54.1 ± 0.5 Hz/°C. Dividing these coefficients by the Larmor frequency of ^{23}Na at 9.4 T (107.07 Hz/PPM) gives values of −0.48 ± 0.01 PPM/°C for the gel sample and −0.51 ± 0.01 PPM/°C for the solution. These coefficients are 50 times more sensitive than the coefficient for water protons!

In addition, we undertook an investigation of the sodium relaxation properties as a function of temperature. T_1 was computed for the agarose gel and solution samples at four different temperatures, 24, 34, 39, and 44°C. Biexponential T_2 was measured for the gel at these same temperatures. Table 1 summarizes the effect of temperature on relaxation times. Immediately obvious are the extremely short T_1's and T_2's in $Na_4HTm[DOTP]$, owing to the efficient relaxation mechanisms of the unpaired electrons of the thulium present. This is in addition to the already strong quadrupolar relaxation mecha-

TABLE 1
Relaxation Time Measurements for the Solution and Agarose Gel Samples

Measurement	24°C	34°C	39°C	44°C
T_1 $Na_4HTm[DOTP]$ agarose (ms)	3.05 ± .01	3.90 ± .01	4.37 ± .01	4.97 ± .02
T_1 $Na_4HTm[DOTP]$ solution (ms)	3.13 ± .02	4.01 ± .02	4.49 ± .03	5.02 ± .02
T_1 NaCl in agarose (ms)	20.0 ± .07			
T_1 NaCl solution (ms)	60.0 ± .50			
T_{2f} $Na_4HTm[DOTP]$ agarose (ms)	1.34 ± .15	1.46 ± .11	1.65 ± .15	2.00 ± .09
T_{2s} $Na_4HTm[DOTP]$ agarose (ms)	3.01 ± .05	3.64 ± .08	4.27 ± .07	4.92 ± .06
T_{2f} NaCl in agarose (ms)	4.2 ± .07			
T_{2s} NaCl in agarose (ms)	50.8 ± 1.1			

Note. Relaxation times are expressed as ms ± 1 standard deviation.

nism of the sodium nuclei. The dominant mechanism for further T_1 and T_2 relaxation rate enhancement is the pseudo-contact interaction generated by dipolar fields by the metal electrons and felt by the neighboring sodium (*20*).

Both T_1 and T_2 increased with a rise in temperature as is predicted by Bloembergen–Purcell–Pound theory, where expressions for both $1/T_1$ and $1/T_2$, in this motional regime, are proportional to 1/temperature (*21*). However, contrary to the high sensitivity the chemical shift frequency elicits with temperature, the relaxation rates do not change significantly per degree. Over a 20° temperature range, the T_1 increased nearly 2 ms for both the gel and the solution.

In conclusion, we have characterized a temperature-sensitive sodium chemical shift frequency for $Na_4HTm[DOTP]$. This temperature-dependent chemical shift coefficient is on the order of 0.5 PPM/°C, 50 times more sensitive than the temperature-dependent chemical shift coefficient of water protons. Additionally, a T_1 dependence of 0.1 ms/°C was found. Linewidths of the several spectra were measured and found to be equal at each temperature. The linewidth of a line resulting from a pulse–acquire sequence decays with T_2^*, not T_2. Even as T_{2f} and T_{2s} are increased with temperature, the T_2^* may be so short that its effect from temperature may not have influenced the linewidth. The extreme sensitivity of the sodium chemical shift may have many applications, both in living systems and in magnetic resonance hardware considerations. Proton MR of $Tm[DOTP]^{5-}$ has already been investigated for use as an *in vivo* MRI "thermometer" (*11*). We anticipate the future use of the sodium signal as a complement. However, a potential obstacle to achieving this is the strong possibility that pH variance and DOTP binding site competition by calcium and other cations may alter the temperature-dependent chemical shift coefficient (*11*).

With this in mind, the unique properties of $Na_4HTm[DOTP]$ may enable its usage in the measurement of heat deposition in tissue phantoms as a result of the MRI experiment. During the MRI experiment, radiofrequency (RF) power is absorbed by the subject, which in turn may lead to heating (*22*). Numerous calculations and simulations predict that, at higher fields, the issue of RF heating becomes much more severe (*23, 24*). However, there are no high-resolution experimental methods for measuring power deposition in tissue or a tissue phantom during MRI examination. The ^{23}Na temperature-dependent chemical shift produces a phase shift governed by $\Delta\omega\tau$, where $\Delta\omega$ is the frequency shift and τ is the evolution time. While keeping τ short to preserve the signal, the large $\Delta\omega$ allows the measurement of small temperature differences through the phase shift. The full expression for the phase shift resulting from a change in chemical shift is

$$\Delta\phi = 360 \cdot K \cdot (\gamma B_0) \cdot \mathrm{TE} \cdot \Delta T,$$

where K is the temperature-dependent chemical shift coefficient, TE is the echo time in a gradient echo pulse sequence, and ΔT is the temperature difference. This yields for ^{23}Na at 4.0T (45 MHz) a 1° phase shift representing a temperature change of only 0.06°C! It should be noted here that the echo time plays a crucial role in determining the sensitivity of this measurement. Species with longer T_2's will allow for a longer echo time to be used. Consequently, this same technique could possibly be accomplished using water, employing its -0.01 PPM/°C temperature-dependent chemical shift and using an echo time equal to T_2.

By monitoring the ^{23}Na chemical shift in an agarose tissue phantom containing 40 mM $Na_4HTm[DOTP]$ and creating temperature maps based on the phase of the observed signal, one will be able to test both aged and novel MRI coils for RF absorption violations and local electric field hot spots. Hot spots normally arise due to a malfunctioning of a coil component or failure to adequately distribute capacitance, thereby creating large electric field densities in and around the coil. The choice of which substance to use in the analysis of RF heating patterns will ultimately be determined by the coil. For an RF coil tuned to ^{23}Na, imaging the ^{23}Na from the $Na_4HTm[DOTP]$ doped phantom would be an appropriate choice. An RF coil tuned to ^{1}H would require using a phantom that possessed protons which exhibited temperature-dependent chemical shift and/or relaxation characteristics. This could be water, paramagnetic doped water, or the protons of a paramagnetic shift reagent such as $Na_4HTm[DOTP]$. Experiments in these several directions are currently underway in our laboratory. Using doped agarose gels to evaluate coil performance and safety may ultimately prevent both injuries to patients as a result of the MRI experiment and instrumentation failure.

ACKNOWLEDGMENTS

This work was performed at an NIH Resource Center supported by Grants RR02305 and R01 AR45242-01. We thank Dr. Suzanne Wherli for assistance with the NMR measurements and Dr. Michael Shapiro for helpful discussions.

REFERENCES

1. D. Lebihan, J. Delannoy, and R. L. Levin, Temperature mapping with MR imaging of molecular diffusion: application to hyperthermia, *Radiology* **171,** 853–857 (1989).
2. D. L. Carter, J. R. MacFall, S. T. Clegg, X. Wan, D. M. Prescott, H. C. Charles, and T. V. Samulski, Magnetic resonance thermometry during hyperthermia for human high-grade sarcoma, *Int. J. Radiat. Oncol. Biol. Phys.* **40,** 815–822 (1998).
3. N. McDannold, K. Hynynen, D. Wolf, G. Wolf, and F. Jolesz, MRI evaluation of thermal ablation of tumors with focused ultrasound, *J. Magn. Reson. Imaging* **8,** 91–100 (1998).
4. W. Wlodarczyk, R. Boroschewski, M. Hentschel, P. Wust, G. Monich, and R. Felix, Three-dimensional monitoring of small temperature changes for therapeutic hyperthermia using MR, *J. Magn. Reson. Imaging* **8,** 165–174 (1998).
5. K. Kuroda, Y. Suzuki, Y. Ishihara, K. Okamoto, and Y. Suzuki, Temperature mapping using water proton chemical shift obtained

with 3D-MRSI: Feasability *in-vivo, Magn. Reson. Med.* **35,** 20–29 (1996).

6. M. Hayashi, S. Hanakawa, M. Senda, and Y. Takahara, Evaluation of the thigh muscles after knee exercise on a Cybex II, *Acta Med. Okayama* **52,** 155–160 (1998).
7. F. Bertsch, J. Mattner, M. K. Stehling, U. Muller-Lisse, M. Peller, R. Loeffler, J. Weber, K. Messmer, W. Wilmanns, R. Issels, and M. Reiser, Non-invasive temperature mapping using MRI: Comparison of two methods based on chemical shift and T_1 relaxation, *Magn. Reson. Imaging* **16,** 393–403 (1998).
8. J. R. MacFall, D. M. Prescott, H. C. Charles, and T. V. Samulski, ^{1}H MRI phase thermometry *in vivo* in canine brain, muscle, and tumor tissue, *Med. Phys.* **23,** 1775–1782 (1996).
9. I. R. Young, J. W. Hand, A. Oatridge, M. V. Prior, and G. R. Forse, Further observations on the measurement of tissue T_1 to monitor temperature *in-vivo* by MRI, *Magn. Reson. Med.* **31,** 342–345 (1994).
10. J. Delannoy, C. N. Chen, R. Turner, R. L. Levin, and D. Lebihan, Noninvasive temperature imaging using diffusion MRI, *Magn. Reson. Med.* **19,** 333–339 (1991).
11. C. S. Zuo, K. R. Metz, Y. Sun, and A. D. Sherry, NMR temperature measurements using a paramagnetic lanthanide complex, *J. Magn. Reson.* **133,** 53–60 (1998).
12. G. D. Waiter and M. A. Foster, Lanthanide-EDTA doped agarose gels for use in NMR imaging phantoms, *Magn. Reson. Imaging* **15,** 929–938 (1997).
13. C. S. Zuo, J. L. Bowers, K. R. Metz, T. Nosaka, A. D. Sherry, and M. E. Clouse, $Tm[DOTP]^{5-}$: A substance for NMR temperature measurements *in vivo*, *Magn. Reson. Med.* **36,** 955–959 (1996).
14. S. Aime, M. Botta, M. Fasano, E. Terreno, P. Kinchesh, L. Calabi, and L. Paleari, A new ytterbium chelate as contrast agent in chemical shift imaging and temperature sensitive probe for MR spectroscopy, *Magn. Reson. Med.* **35,** 648–651 (1996).
15. T. Frenzel, K. Roth, S., Kossler, B. Raduchel, H. Bauer, J. Platzek, and H. J. Weinmann, Noninvasive temperature measurement *in vivo* using a temperature-sensitive lanthanide complex and ^{1}H magnetic resonance spectroscopy, *Magn. Reson. Med.* **35,** 364–369 (1996).
16. N. Bansal, M. J. Germann, V. Seshan, G. T. Shires, C. R. Malloy, and A. D. Sherry, Thulium 1,4,7,10-tetraazacyclododecane-1,4,7,10- tetrakis(methylene phosphonate) as a ^{23}Na shift reagent for the *in-vivo* rat liver, *Biochemistry* **32,** 5638–5643 (1993).
17. G. Jaccard, S. Wimperis, and G. Bodenhausen, Multiple quantum NMR spectroscopy of $S = \frac{3}{2}$ spins in isotropic phase: A new probe for multiexponential relaxation, *J. Chem. Phys.* **85,** 6282–6293 (1986).
18. J. Pekar and J. S. Leigh, Detection of bi-exponential relaxation in sodium-23 facilitated by double quantum filtering, *J. Magn. Reson.* **69,** 582–584 (1986).
19. U. Duvvuri, J. H. Kaufman, S. D. Patel, L. Bolinger, J. B. Kneeland, J. S. Leigh, and R. Reddy, Sodium multiple quantum spectroscopy of articular cartilage: Effects of mechanical compression, *Magn. Reson. Med.* **40,** 370–375 (1998).
20. N. Bloembergen and L. O. Morgan, Proton relaxation times in paramagnetic solutions. Effects of electron spin relaxation, *J. Chem. Phys.* **34,** 842–850 (1961).
21. N. Bloembergen, E. M. Purcell, and R. V. Pound, Relaxation effects in nuclear magnetic resonance absorption, *Phys. Rev.* **73,** 679–718 (1948).
22. C. N. Chen and D. I. Hoult, The visualization of RF probe electric fields, *Magn. Reson. Med.* **29,** 386–390 (1993).
23. C. M. Collins, S. Z. Li, and M. B. Smith, SAR and B_1 field distributions in a heterogeneous human head model within a birdcage coil, *Magn. Reson. Med.* **40,** 847–856 (1998).
24. J. M. Jin and J. Chen, On the SAR and field inhomogeneity of birdcage coils loaded with the human head, *Magn. Reson. Med.* **38,** 953–963 (1997).